

Further probing the neutron star equation of state via frequency deviations in universal relations

Georgios Lioutas,^{a,b,*} Andreas Bauswein^{a,c} and Nikolaos Stergioulas^d

^a*GSI Helmholtzzentrum für Schwerionenforschung,
Planckstraße 1, 64291 Darmstadt, Germany*

^b*Department of Physics and Astronomy, Ruprecht-Karls-Universität Heidelberg,
Im Neuenheimer Feld 226, 69120 Heidelberg, Germany*

^c*Helmholtz Research Academy Hesse for FAIR (HFHF), GSI Helmholtz Center for Heavy Ion Research,
Campus 64291 Darmstadt, Germany*

^d*Department of Physics, Aristotle University of Thessaloniki,
54124 Thessaloniki, Greece*

E-mail: g.lioutas@gsi.de, a.bauswein@gsi.de, niksterg@auth.gr

Gravitational wave observations of neutron star systems are very important to constrain the neutron star equation of state. Empirical relations between the characteristics of the gravitational wave signal and stellar parameters of static stars are employed to connect the observable signal with the underlying physics. Here, we consider empirical relations linking the frequency of the fundamental quadrupolar fluid mode in isolated neutron stars and the dominant post-merger oscillation frequency in binary neutron star mergers to the radius of static stars. We consider how individual data points distribute with respect to the corresponding fit to all points for both neutron star systems. We find that the deviations from the respective fit follow a very similar behavior in these two systems. We outline how to employ the scatter of the points to more accurately relate the radius and the tidal deformability.

*FAIR next generation scientists - 7th Edition Workshop (FAIRness2022)
23-27 May 2022
Paralia (Pieria, Greece)*

*Speaker

1. Introduction

Gravitational waves (GWs) produced by fluid oscillations in neutron star (NS) systems carry information about the stellar structure. A number of GW asteroseismology relations have been proposed, which link the frequency of the GW signal to stellar properties of static stars. For instance, the frequency of the fundamental quadrupolar fluid mode (f -mode) in isolated NSs has been related to various stellar parameters [1–4]. Similarly, many relations have been proposed involving the frequency of the dominant fluid oscillation in binary neutron star (BNS) merger remnants (see e.g. [5–11]). Such relations can help to infer stellar properties of NSs, which are uniquely linked to the underlying equation of state (EOS). Hence, these empirical relations provide the opportunity to constrain the high-density EOS, which is only partially known [12–17], through GW observations.

This study focuses on fluid modes from two very distinct NS systems, the f -mode in non-rotating, isolated NSs and the dominant post-merger oscillation frequency of BNS merger remnants. For both systems, we consider empirical relations between the oscillation frequencies and the radii of static stars. We review the exact way in which data points, i.e. stellar configurations modeled by different EOSs, distribute with respect to a fit to all data following the analysis in [18]. We demonstrate that data points scatter in a very similar way when comparing relations referring to isolated stars and BNS merger remnants, respectively. We outline how this scatter can be related to the EOS and in particular to the tidal Love number k_2 [19–21].

2. Setup and data sets

2.1 Isolated stars

We study the f -mode in cold, isolated, non-rotating NSs based on a perturbative approach. The f -mode pulsation frequencies, which we denote by f_{pert} , are computed with the code initially presented in [22]. In this work, we focus on stellar models with a gravitational mass of $1.6 M_{\odot}$.

2.2 Binary neutron star mergers

We extract the dominant post-merger GW frequency, which we denote by f_{peak} , from 3D simulations of BNS mergers. The simulations are carried out with a smoothed particle hydrodynamics code (see [6, 23–25] for more details on the code and simulations), which employs the conformal flatness condition [26, 27]. In this work, we focus on $1.35 + 1.35 M_{\odot}$ binary systems. A more extensive study, which considers in addition systems with different total binary masses, can be found in [18].

2.3 Equations of state

In this study, we discuss perturbative calculations, as well as BNS merger simulations, for a set of 19 EOSs. These EOSs are ALF2 [28, 29], APR [30], BHBLP [31], BSK20 [32], BSK21 [32], DD2 [33, 34], DD2F [34–36], DD2Y [37, 38], LS220 [39], LS375 [39], GS2 [40], NL3 [33, 41], SFHO [42], SFHOY [37, 38], SFHX [42], SLY4 [43], TM1 [44, 45], TMA [45, 46], WFF2 [47]. This collection of EOSs covers a wide range in the gravitational mass, M , versus radius, R , parameter space (see Fig. 1 in [18]).

3. Frequency deviations and relation to the tidal Love number k_2

Figure 1 displays empirical relations between the frequency and the radius for the two different systems that we consider, i.e. isolated NSs and BNS merger remnants. Panel 1a shows the perturbative frequencies of $1.6 M_\odot$ stars, $f_{\text{pert},1.6}$, as a function of the radius of static NSs with the same mass, $R_{1.6}$. In panel 1b we plot the dominant post-merger frequencies referring to $1.35 + 1.35 M_\odot$ binary systems, f_{peak} , versus the same independent variable as in panel 1a, namely $R_{1.6}$. Each data point is a stellar model described by a different EOS. The green line in each panel represents a second order fit to all the respective data. The expressions for the fits in panels 1a and 1b can be found in Tables V and III in [18], respectively, alongside the average and maximum deviation of the data points from the respective fit measured in Hz.

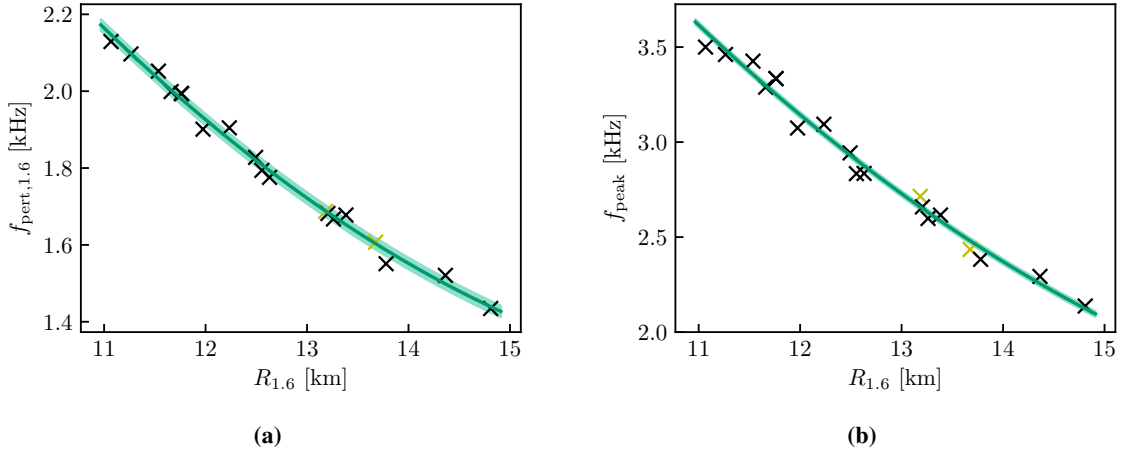


Figure 1: Perturbative f -mode frequencies for $1.6 M_\odot$ configurations (left panel) and dominant post-merger oscillation frequencies for $1.35 + 1.35 M_\odot$ binary systems (right panel) as a function of the radius of static $1.6 M_\odot$ stars. For the explanation of the colors, see the main text. Figures taken from [18].

We focus on individual data points (i.e. EOSs) and classify them based on how they are positioned with respect to the corresponding fits in both panels in Fig. 1. A simple criterion would be to examine whether an EOS lies above or below the fit in both plots. However, such an approach is not accurate for points very close to the fits. For instance, constructing the fit based on a different EOS sample or employing another functional form for the relation can influence whether a data point lies above or below the fit, particularly for points which lie rather close to it. Hence, we introduce green shaded bands with a total width of 30 Hz around each fit to more carefully account for such points¹. Data points which lie above or below the respective fit in both panels are depicted with black symbols. Similarly, we employ black symbols to denote data points which lie within the green shaded band around the fits in both panels, i.e. they lie very close to the fit for both the relation involving f_{pert} , as well as the relation with f_{peak} . We classify EOSs as outliers if they simultaneously lie on opposite sides of the respective relations in these two panels and, in addition, outside the green shaded band in at least one of the diagrams. Outliers are shown with yellow symbols in Fig. 1.

¹We note that the average deviation of data points from the fit in panel 1b is 48 Hz (see Table III in [18]). Hence, most data points are more than 15 Hz away from the fit in panel 1b, namely they lie outside the green shaded band.

Remarkably, based on the introduced classification, 17 out of 19 data points distribute in the same way with respect to the corresponding fits when examining the two panels in Fig. 1 side by side. This behavior is rather unexpected considering that the relations in the two panels in Fig. 1 refer to two very different systems. Perturbative frequencies f_{pert} (panel 1a) are computed for cold, non-rotating, isolated NSs, while the post-merger frequencies f_{peak} (panel 1b) correspond to the dominant oscillation in a hot, rapidly rotating and massive merger remnant. In this work, we discuss only $1.6 M_{\odot}$ isolated NSs and $1.35 + 1.35 M_{\odot}$ binary systems. However, a more extensive analysis reveals that similar agreement is found when considering various pairs of relations constructed based on isolated NSs or binary systems with different masses than those discussed here, as well as employing the fifth-root of the tidal deformability² $\Lambda^{1/5}$ as the independent variable instead of R (see Table IV and relevant discussion in [18]).

The striking agreement in the way that points scatter around the respective fits for both isolated NSs and BNS merger remnants implies that the deviations of the data points from the corresponding frequency relations (hereafter called frequency deviations) are influenced by an underlying mechanism. The only connection between the two physical systems is the EOS, which suggests that the frequency deviations carry additional information about the EOS³.

A key element to better understand frequency deviations is the observation that the perturbative frequencies correlate with the tidal deformability extremely tightly (see Figs. 3 and 7 and relevant discussion in [18], as well as [4, 48]). In particular, for stellar models with a fixed mass described by different EOSs, the relation between f_{pert} and $\Lambda^{1/5}$ displays minimal scatter. Hence, the deviations in a frequency versus radius relation can be directly associated to the data scatter in a $\Lambda^{1/5}$ versus R diagram. Considering the definition of the tidal deformability, this suggests that the frequency deviations can be traced back to the tidal Love number k_2 .

The tidal Love number k_2 scales with the inverse compactness R/M (see tidal deformability definition and e.g. [49]). We show this correlation in the upper panel of Fig. 2. The green curve is a second-order fit to the data and is the same in all panels, while the gray shaded band depicts the maximum deviation from the fit in each panel. Evidently, the data points exhibit some sizable scatter around the relation. Based on the previous discussion, the scatter in the k_2 versus R/M relation is directly related to the deviations of the data points from the respective fit in frequency versus radius diagrams.

We quantify frequency deviations by measuring how much each data point deviates from the respective fit in terms of Hz. In the case of panels 1a and 1b, we denote frequency deviations as $\delta_R f_{\text{pert},1.6}$ and $\delta_R f_{\text{peak}}$, respectively. Employing $\delta_R f_{\text{pert},1.6}$ practically removes the scatter exhibited in the upper panel of Fig. 2. This is explicitly shown in the middle panel of Fig. 2, where we present the quantity $k_2 - b \delta_R f_{\text{pert},1.6}$ as a function of R/M . Here $b = -0.2206 \text{ kHz}^{-1}$ is determined by fitting the deviations in the upper panel in Fig. 2. Evidently, employing $\delta_R f_{\text{pert},1.6}$ significantly reduces the maximum deviation of the data points from the second-order fit (i.e. the gray shaded area around the green curve). We emphasize once more that each data point refers to a different

²The tidal deformability is defined as $\Lambda = \frac{2}{3} k_2 \left(\frac{c^2 R}{GM} \right)^5$, where c is the speed of light and G is the gravitational constant.

³We refer to the discussion in Section IIIA in [18] for a number of arguments supporting that the scatter in frequency relations is influenced by the high-density EOS.

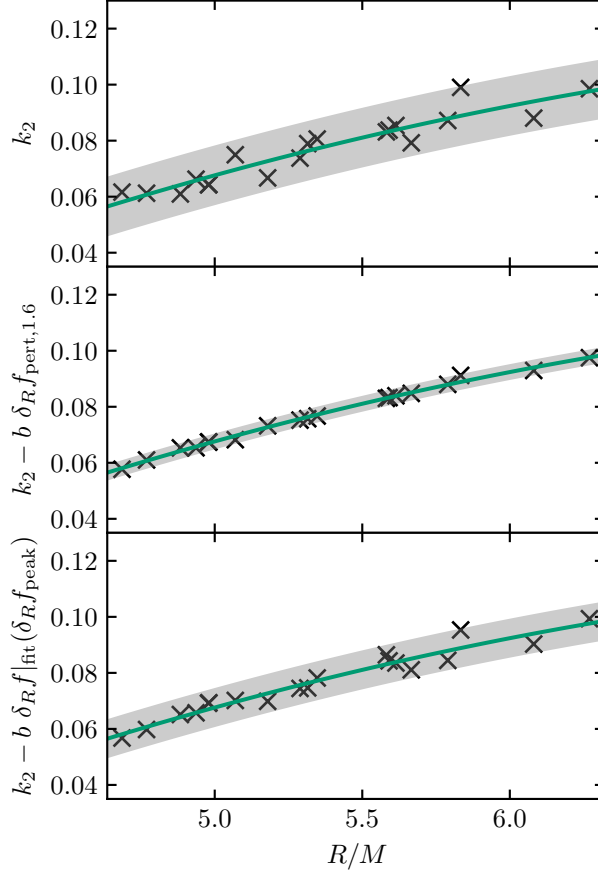


Figure 2: In the upper panel we display k_2 versus the inverse compactness. In the middle and lower panels we correct k_2 based on frequency deviations referring to isolated NSs ($\delta_R f_{\text{pert},1.6}$) and the dominant post-merger oscillation ($\delta_R f_{\text{peak}}$), respectively. Figure taken from [18].

EOS, which highlights the more pronounced EOS-insensitive nature of the $k_2 - b \delta_R f_{\text{pert},1.6}$ versus R/M relation, compared to the $k_2(R/M)$ fit.

We present a similar analysis based on the frequency deviations of merger remnants, $\delta_R f_{\text{peak}}$, in the lower panel in Fig. 2. For this purpose, a linear relation between $\delta_R f_{\text{pert},1.6}$ and $\delta_R f_{\text{peak}}$ (see Fig. 10 in [18]), denoted as $\delta_R f|_{\text{fit}}(\delta_R f_{\text{peak}})$, is employed. Such a correlation is motivated by the fact that data points scatter in a very similar way around the respective fits in Fig. 1. Employing $\delta_R f_{\text{peak}}$ reduces the maximum deviation from the second-order fit between k_2 and R/M by 36% compared to the upper panel in Fig. 2.

We note that, in principle, measuring frequency deviations might be challenging. However, determining the sign of $\delta_R f_{\text{pert}}$ is already sufficient to decrease the error in estimating k_2 by half, because it reveals whether the corresponding data point is located above or below the $k_2(R/M)$ relation. Overall, it is evident that employing frequency deviations leads to more precise estimates for k_2 and, thus, enables to more accurately relate the radius to the tidal deformability. Considering that both R and Λ are uniquely related to the EOS, frequency deviations offer the potential for stricter EOS constraints.

4. Conclusions

In this work, we closely examine how data points distribute with respect to the fit to all data in GW frequency versus radius diagrams. We consider frequencies from two very different NS systems, namely the f -mode oscillation in cold, non-rotating, isolated NSs and the dominant post-merger oscillation in hot, rapidly rotating, massive BNS merger remnants. We discuss how the data points deviate from the respective fits in a strikingly similar way when comparing these two NS systems side by side. Furthermore, we outline how these deviations can be traced back to the tidal Love number k_2 and explicitly review how the deviations can be employed to obtain better estimates for k_2 and, subsequently, break the degeneracy between R , Λ and k_2 . A more extensive analysis, covering a broader range of masses and additional types of relations, can be found in [18].

Acknowledgments

G.L. and A.B. acknowledge support by the European Research Council (ERC) under the European Union’s Horizon 2020 research and innovation program under grant agreement No. 759253, as well as by the Deutsche Forschungsgemeinschaft (DFG, German Research Foundation) - Project-ID 138713538 - SFB 881 (“The Milky Way System”, subproject A10). A.B. acknowledges support by DFG - Project-ID 279384907 - SFB 1245 and by the State of Hesse within the Cluster Project ELEMENTS. N.S. acknowledges support by the ARIS facility of GRNET in Athens (SIMGRAV, SIMDIFF and BNSMERGE allocations) and the “Aristoteles Cluster” at AUTH, as well as by the COST actions CA16214 “PHAROS”, CA16104 “GWVerse”, CA17137 “G2Net” and CA18108 “QG-MM”. N.S. gratefully acknowledges the Italian Istituto Nazionale di Fisica Nucleare (INFN), the French Centre National de la Recherche Scientifique (CNRS) and the Netherlands Organization for Scientific Research, for the construction and operation of the Virgo detector and the creation and support of the EGO consortium.

References

- [1] N. Andersson and K.D. Kokkotas, *Towards gravitational wave asteroseismology*, *Mon. Not. R. Astron. Soc* **299** (1998) 1059 [[gr-qc/9711088](#)].
- [2] L.K. Tsui and P.T. Leung, *Universality in quasi-normal modes of neutron stars*, *Mon. Not. R. Astron. Soc* **357** (2005) 1029 [[gr-qc/0412024](#)].
- [3] H.K. Lau, P.T. Leung and L.M. Lin, *Inferring Physical Parameters of Compact Stars from their f -mode Gravitational Wave Signals*, *Astrophys. J.* **714** (2010) 1234 [[0911.0131](#)].
- [4] T.K. Chan, Y.H. Sham, P.T. Leung and L.M. Lin, *Multipolar universal relations between f -mode frequency and tidal deformability of compact stars*, *Phys. Rev. D* **90** (2014) 124023 [[1408.3789](#)].
- [5] A. Bauswein and H.T. Janka, *Measuring Neutron-Star Properties via Gravitational Waves from Neutron-Star Mergers*, *Phys. Rev. Lett.* **108** (2012) 011101 [[1106.1616](#)].

- [6] A. Bauswein, H.T. Janka, K. Hebeler and A. Schwenk, *Equation-of-state dependence of the gravitational-wave signal from the ring-down phase of neutron-star mergers*, *Phys. Rev. D* **86** (2012) 063001 [1204.1888].
- [7] K. Takami, L. Rezzolla and L. Baiotti, *Spectral properties of the post-merger gravitational-wave signal from binary neutron stars*, *Phys. Rev. D* **91** (2015) 064001 [1412.3240].
- [8] S. Bernuzzi, T. Dietrich and A. Nagar, *Modeling the Complete Gravitational Wave Spectrum of Neutron Star Mergers*, *Phys. Rev. Lett.* **115** (2015) 091101 [1504.01764].
- [9] S. Vretinaris, N. Stergioulas and A. Bauswein, *Empirical relations for gravitational-wave asteroseismology of binary neutron star mergers*, *Phys. Rev. D* **101** (2020) 084039 [1910.10856].
- [10] S. Blacker, N.-U.F. Bastian, A. Bauswein, D.B. Blaschke, T. Fischer, M. Oertel et al., *Constraining the onset density of the hadron-quark phase transition with gravitational-wave observations*, *Phys. Rev. D* **102** (2020) 123023 [2006.03789].
- [11] A. Bauswein and N. Stergioulas, *Spectral classification of gravitational-wave emission and equation of state constraints in binary neutron star mergers*, *Journal of Physics G Nuclear Physics* **46** (2019) 113002 [1901.06969].
- [12] J.M. Lattimer and M. Prakash, *Neutron star observations: Prognosis for equation of state constraints*, *Phys. Rep.* **442** (2007) 109 [astro-ph/0612440].
- [13] J.M. Lattimer, *The Nuclear Equation of State and Neutron Star Masses*, *Annual Review of Nuclear and Particle Science* **62** (2012) 485 [1305.3510].
- [14] F. Özel and P. Freire, *Masses, Radii, and the Equation of State of Neutron Stars*, *Annu. Rev. Astron. Astrophys.* **54** (2016) 401 [1603.02698].
- [15] M. Oertel, M. Hempel, T. Klähn and S. Typel, *Equations of state for supernovae and compact stars*, *Reviews of Modern Physics* **89** (2017) 015007 [1610.03361].
- [16] S. Lalit, M.A.A. Mamun, C. Constantinou and M. Prakash, *Dense matter equation of state for neutron star mergers*, *European Physical Journal A* **55** (2019) 10 [1809.08126].
- [17] K. Hebeler, *Three-nucleon forces: Implementation and applications to atomic nuclei and dense matter*, *Phys. Rep* **890** (2021) 1 [2002.09548].
- [18] G. Lioutas, A. Bauswein and N. Stergioulas, *Frequency deviations in universal relations of isolated neutron stars and postmerger remnants*, *Phys. Rev. D* **104** (2021) 043011 [2102.12455].
- [19] T. Hinderer, *Tidal Love Numbers of Neutron Stars*, *Astrophys. J.* **677** (2008) 1216 [0711.2420].

- [20] T. Hinderer, B.D. Lackey, R.N. Lang and J.S. Read, *Tidal deformability of neutron stars with realistic equations of state and their gravitational wave signatures in binary inspiral*, *Phys. Rev. D* **81** (2010) 123016 [0911.3535].
- [21] T. Damour and A. Nagar, *Effective one body description of tidal effects in inspiralling compact binaries*, *Phys. Rev. D* **81** (2010) 084016 [0911.5041].
- [22] G. Lioutas and N. Stergioulas, *Universal and approximate relations for the gravitational-wave damping timescale of f -modes in neutron stars*, *General Relativity and Gravitation* **50** (2018) 12 [1709.10067].
- [23] R. Oechslin, S. Rosswog and F.-K. Thielemann, *Conformally flat smoothed particle hydrodynamics application to neutron star mergers*, *Phys. Rev. D* **65** (2002) 103005 [gr-qc/0111005].
- [24] R. Oechslin, H.T. Janka and A. Marek, *Relativistic neutron star merger simulations with non-zero temperature equations of state. I. Variation of binary parameters and equation of state*, *Astron. Astrophys.* **467** (2007) 395 [astro-ph/0611047].
- [25] A. Bauswein, R. Oechslin and H.T. Janka, *Discriminating strange star mergers from neutron star mergers by gravitational-wave measurements*, *Phys. Rev. D* **81** (2010) 024012 [0910.5169].
- [26] J. Isenberg and J. Nester, *Canonical Gravity*, in *General Relativity and Gravitation. Vol. 1. One hundred years after the birth of Albert Einstein*. Edited by A. Held. New York, vol. 1, p. 23, Jan., 1980.
- [27] J.R. Wilson, G.J. Mathews and P. Marronetti, *Relativistic numerical model for close neutron-star binaries*, *Phys. Rev. D* **54** (1996) 1317 [gr-qc/9601017].
- [28] M. Alford, M. Braby, M. Paris and S. Reddy, *Hybrid stars that masquerade as neutron stars*, *Astrophys. J* **629** (2005) 969.
- [29] J.S. Read, B.D. Lackey, B.J. Owen and J.L. Friedman, *Constraints on a phenomenologically parametrized neutron-star equation of state*, *Phys. Rev. D* **79** (2009) 124032.
- [30] A. Akmal, V.R. Pandharipande and D.G. Ravenhall, *Equation of state of nucleon matter and neutron star structure*, *Phys. Rev. C* **58** (1998) 1804.
- [31] S. Banik, M. Hempel and D. Bandyopadhyay, *New hyperon equations of state for supernovae and neutron stars in density-dependent hadron field theory*, *Astrophys. J., Suppl. Ser.* **214** (2014) 22.
- [32] S. Goriely, N. Chamel and J.M. Pearson, *Further explorations of Skyrme-Hartree-Fock-Bogoliubov mass formulas. XII. Stiffness and stability of neutron-star matter*, *Phys. Rev. C* **82** (2010) 035804.
- [33] M. Hempel and J. Schaffner-Bielich, *A statistical model for a complete supernova equation of state*, *Nucl. Phys. A* **837** (2010) 210.

- [34] S. Typel, G. Röpke, T. Klähn, D. Blaschke and H.H. Wolter, *Composition and thermodynamics of nuclear matter with light clusters*, *Phys. Rev. C* **81** (2010) 015803.
- [35] S. Typel, *Relativistic model for nuclear matter and atomic nuclei with momentum-dependent self-energies*, *Phys. Rev. C* **71** (2005) 064301.
- [36] D. Alvarez-Castillo, A. Ayriyan, S. Benic, D. Blaschke, H. Grigorian and S. Typel, *New class of hybrid eos and bayesian $m - r$ data analysis*, *European Physical Journal A* **52** (2016) 69.
- [37] M. Fortin, M. Oertel and C. Providência, *Hyperons in hot dense matter: what do the constraints tell us for equation of state?*, *Publ. Astron. Soc. Aust.* **35** (2018) .
- [38] M. Marques, M. Oertel, M. Hempel and J. Novak, *New temperature dependent hyperonic equation of state: Application to rotating neutron star models and I-Q relations*, *Phys. Rev. C* **96** (2017) 045806.
- [39] J.M. Lattimer and F. Douglas Swesty, *A generalized equation of state for hot, dense matter*, *Nuclear Physics A* **535** (1991) 331.
- [40] G. Shen, C.J. Horowitz and S. Teige, *New equation of state for astrophysical simulations*, *Phys. Rev. C* **83** (2011) 035802.
- [41] G.A. Lalazissis, J. König and P. Ring, *New parametrization for the lagrangian density of relativistic mean field theory*, *Phys. Rev. C* **55** (1997) 540.
- [42] A.W. Steiner, M. Hempel and T. Fischer, *Core-collapse supernova equations of state based on neutron star observations*, *Astrophys. J.* **774** (2013) 17.
- [43] F. Douchin and P. Haensel, *A unified equation of state of dense matter and neutron star structure*, *Astron. Astrophys.* **380** (2001) 151.
- [44] Y. Sugahara and H. Toki, *Relativistic mean-field theory for unstable nuclei with non-linear σ and ω terms*, *Nuclear Physics A* **579** (1994) 557.
- [45] M. Hempel, T. Fischer, J. Schaffner-Bielich and M. Liebendörfer, *New Equations of State in Simulations of Core-collapse Supernovae*, *Astrophys. J.* **748** (2012) 70.
- [46] H. Toki, D. Hirata, Y. Sugahara, K. Sumiyoshi and I. Tanihata, *Relativistic many body approach for unstable nuclei and supernova*, *Nuclear Physics A* **588** (1995) 357.
- [47] R.B. Wiringa, V. Fiks and A. Fabrocini, *Equation of state for dense nucleon matter*, *Phys. Rev. C* **38** (1988) 1010.
- [48] D.-H. Wen, B.-A. Li, H.-Y. Chen and N.-B. Zhang, *GW170817 implications on the frequency and damping time of f -mode oscillations of neutron stars*, *Phys. Rev. C* **99** (2019) 045806 [1901.03779].
- [49] S. De, D. Finstad, J.M. Lattimer, D.A. Brown, E. Berger and C.M. Biwer, *Tidal Deformabilities and Radii of Neutron Stars from the Observation of GW170817*, *Phys. Rev. Lett.* **121** (2018) 091102 [1804.08583].